Multipath Model Order Selection for Non-Line Of Sight Radar Localization in Urban Environment

Ba-Huy Pham[1,2], Olivier Rabaste[1], Jonathan Bosse[1], Israel Hinostroza[2], Thierry Chonavel[3]
[1] DEMR, ONERA, Université Paris-Saclay, F-91123 Palaiseau, France
[2] SONDRA, CentraleSupelec, Université Paris-Saclay, F-91192 Gif-sur-Yvette, France
[3] IMT Atlantique, Lab-STICC, UMR CNRS 6285, F-29238 Brest, France

***Abstract*—In an urban environment, the Non-Line of Sight (NLOS) target position can be determined by exploiting reflections on surrounding building, for instance using Matched Subspace Filter (MSF). However, it has been shown that the MSF output exhibits strong localization ambiguities when different positions share similar paths measurements. This ambiguity phenomenon is all the more exacerbated since the zones in the research domain are generally not illuminated by the same number of paths. In this paper, the well-known Bayesian Information Criterion (BIC) is considered to tackle this problem. Besides, we adopt a multipath selection procedure to select the relevant model for each position under test based on the Orthogonal Least Squares (OLS) sparse approximation algorithm and combine it with BIC as a stopping rule. These solutions, applied on both simulated and experimental data, show better localization results compared to the classical localization scheme.**

***Index Terms*—NLOS target, around-the-corner radar, multipath, matched subspace filter, ambiguities, ray tracing simulation.**

I. Introduction

Non-Line-of-Sight (NLOS) target detection/localization is a quite recent topic in radar, that has strong application potential in the fields of urban surveillance and autonomous vehicles. First feasibility studies were introduced with experimentation in works [1], [2], [3]. Since then, several works have been carried out to further propose localization methods [4], [5], [7], [8].

Unlike most other works on the topic, the localization method of [9], based on Matched Subspace Filter (MSF) [10] enables to formalize the detection and localization problems directly in the target position parameter space [11]. In this approach, each test cell stands for a position (x, y) in the search domain that is represented by a subspace containing several characteristic multipath signal vectors. The MSF estimates the target position by selecting the test cell that yields the maximum likelihood (ML) value for observed data. The major problem is that positions under test may be characterized by one or several paths with similar radar measurements with each other, *i.e.* their corresponding subspaces do share pairwise strongly correlated vectors. In this situation, their likelihood have quite similar values, the target position estimation may be strongly biased. This problem, called *localization ambiguities* in [9], has been discussed in [12] where the authors showed that enriching the model by an additional multipath information such as the Direction-of-Arrival (DoA), at a much lower cost than Doppler, helps to reduce the similarity measurement of characteristic signals between positions and thus improve localization performance. In this paper, we focus on two other factors that contribute to increase localization ambiguities.

First, due to the urban scene configuration, the positions under test may belong to zones that are illuminated by different number of paths, and thus they are represented by subspaces of signals of uneven dimensions. It turns out that the higher the number of paths (*i.e* high subspace dimension), the easier its corresponding model can fit observation, since they provide more degrees of freedom. Hence, this may result in biased estimation of target position. Since ML localization criterion is not sufficient for comparing subspaces of dissimilar dimensions, it is preferable to find another criterion to better handle the trade-off between the goodness-of-fit and the model complexity, for instance via model order selection approach.

Second, the multipath model of each position is often constructed via the ray tracing simulation that is only based on a rough description of the scene geometry [9]. Even though it recovers most possible propagation paths, it tends to exhibit more paths than necessary for both detection and localization problems. It can be observed that the effective number of paths is often smaller than that provided by ray tracing simulation, due to multiple propagation factors, e.g. destructive interference that makes some paths vanish in the measurement. In [9], the authors proved that considering too many paths can degrade detection performance and thus proposed an algorithm to select an optimal number of paths in terms of maximization of the detection probability. Here, the same conclusion can be drawn for the localization problem: too many paths selected for each position model increases risk of localization ambiguities, as described earlier. In order to reduce the number of paths, one needs to know which paths are informative and how many paths are sufficient for the localization problem. One possibility is to rely on observed data to reasonably select the best model for each position.

To summarize, in order to achieve a better localisation performance, it is necessary to solve two problems: first the problem of heterogeneity of the number of paths amongst the different positions, and second the problem of the selection of

the number of paths for a given position.

In this work, we introduce a solution for the localization of a single moving target in NLOS radar in order to solve these two problems. We first show that the localization problem can be seen as a model selection problem. This offers an efficient framework to deal with heterogeneous subspace dimensions. Then the popular Bayesian Information Criterion (BIC) [13] is introduced as a localization criterion that enables to penalize high dimension models that overfit observed data. This allows to solve the first problem. Second, in order to select the number of paths for each position model, we also adopt the BIC. However, since different combinations of paths are possible, the classical procedure requires applying the BIC to a large number of candidate models, which is computationally intractable. To circumvent this drawback, we propose instead the use of the well-known iterative algorithm for sparse approximation Orthogonal Least Squares (OLS) [14], in which the BIC acts as a stopping rule. This enables to reasonably approximate the model selection procedure for each position under test, thus to solve the second problem.

The paper is organized as follows: in Section II, the multipath signal model and the classical detection/localization scheme are introduced. Then the model selection approach for localization problem is presented. In Section III, we present the OLS-BIC multipath selection algorithm. Section IV provides the experimentation setup and localization results on both simulated and real data. In Section V, conclusions are drawn.

In this paper, we adopt the following notations: $(.)^T$, $(.)^H$ denotes transpose and Hermitian transpose, respectively; $\otimes$ denotes the Kronecker product; $\|.\|_2$ denotes the Euclidean norm; $\mathcal{R}(\mathbf{A})$ denotes the range space of matrix $\mathbf{A}$; $\mathbf{P}_A^{\perp}$ denotes the projector onto the orthogonal complement subspace of $\mathbf{A}$. $(\mathbf{A})_i$ stands for the i-th column of $\mathbf{A}$.

II. Problem formulation

A. Received signal model

We consider the problem of locating a single NLOS target with a radar system using a linear array antenna. First, let us suppose a single omni-directional antenna transmitting a narrow-band signal $s(t)$. At the receiver side, we consider a linear array of Q receiving antennas. Multipath propagation is modeled by ray tracing simulation where only specular reflection is considered: diffraction effects are assumed to be negligible for the considered frequency band (cf. Section IV). Under the far field assumption, the signal scattered by a single target at (x, y) and received by the q-th antenna at position vector $\mathbf{x}_q$ is

$$y_q(t) = \sum_{m=1}^{M(x,y)} \alpha_m s(t - \tau_m(x,y)) e^{j\mathbf{k}_{\theta_m(x,y)}^T \mathbf{x}_q} + w_q(t), \quad (1)$$

where $M(x, y)$ denotes the number of multipath returns provided by the ray tracing simulation; $\alpha_m, \tau_m(x, y), \theta_m(x, y)$ refer to the m-th unknown deterministic multipath complex amplitude, round-trip delay and direction-of-arrival (DoA), respectively; $\mathbf{k}_\theta$ is the wave vector in the path receiving direction θ; $w_q(t)$ is the circular complex white Gaussian (CWGN) noise with (known) variance σ^2. In order to save computer time and memory, we apply first the range matched filter on both sides of Eq. (1) so as to discard unused range bins, as suggested in [9]. Correlating both sides of Eq. (1) with $s(t)$ yields MF output:

$$z_q(t) = \sum_{m=1}^{M(x,y)} \alpha_m r(t - \tau_m(x,y)) e^{j\mathbf{k}_{\theta_m(x,y)}^T \mathbf{x}_q} + n_q(t), \quad (2)$$

where $z_q(t)$, $n_q(t)$ and $r(t)$ are obtained by correlation of $y_q(t)$, $w_q(t)$ and $s(t)$ with $s(t)$. Then, sampling each $z_q(t)$ at time period t_s, we obtain the N-dimensional observation vector $\mathbf{z}_q = [z_q(t_s), z_q(2t_s), \ldots, z_q(Nt_s)]^T$. Stacking all Q antenna observation vectors on top of each other, we obtain a single data vector $\mathbf{z}$, that writes

$$\mathbf{z} = \mathbf{R}(x, y)\boldsymbol{\alpha} + \mathbf{n}, \quad (3)$$

where

$$\boldsymbol{\alpha} = [\alpha_1, \alpha_2, \ldots, \alpha_{M(x,y)}]^T \in \mathbb{C}^{M(x,y)\times 1}, \quad (4)$$

$$\mathbf{n} = \left[\mathbf{n}_1^T, \mathbf{n}_2^T, \ldots, \mathbf{n}_Q^T\right]^T \in \mathbb{C}^{QN\times 1}, \quad (5)$$

$$\mathbf{R}(x, y) = \left[\mathbf{r}_1(x, y), \ldots, \mathbf{r}_{M(x,y)}(x, y)\right] \in \mathbb{C}^{QN\times M(x,y)}. \quad (6)$$

The latter denotes the matrix the columns of which stand for multipath signal vectors that span the subspace corresponding to the position (x, y). The m-th multipath signal vector can be written as

$$\mathbf{r}_m(x, y) = \mathbf{r}(\tau_m(x, y)) \otimes \mathbf{a}(\theta_m(x, y)) \in \mathbb{C}^{QN\times 1}, \quad (7)$$

where $\mathbf{a}(\theta_m(x, y)) = \left[e^{j\mathbf{k}_{\theta_m(x,y)}^T \mathbf{x}_1}, \ldots, e^{j\mathbf{k}_{\theta_m(x,y)}^T \mathbf{x}_Q}\right]^T$ denotes the steering vector for the direction $\theta_m(x, y)$.
For the sake of simplicity, the Doppler shift term is neglected in our data model, although we keep in mind that this information has been necessary in the preprocessing stage to cancel the fixed echoes from the received raw signal.

B. Classical localization scheme

The search domain is decomposed into J positions that also corresponds to J test cells. Given the signal model in Eq. (1), the Matched Subspace Filter (MSF), derived from Maximum Likelihood (ML) criterion is applied here for both detection and localization problems. For a test cell (x_j, y_j), the MSF output is given by [9]

$$T_{MSF}(x_j, y_j) = \|\mathbf{P}(x_j, y_j)\mathbf{z}\|_2^2 \underset{\mathcal{H}_0}{\overset{\mathcal{H}_1}{\gtrless}} \lambda, \quad (8)$$

where λ denotes the detection threshold, set according to the desired false alarm rate P_{FA} and

$$\mathbf{P}(x_j, y_j) = \mathbf{R}(x_j, y_j)\left(\mathbf{R}(x_j, y_j)^H \mathbf{R}(x_j, y_j)\right)^{-1} \mathbf{R}(x_j, y_j), \quad (9)$$

is the orthogonal projector onto $\mathcal{R}(\mathbf{R}(x_j, y_j))$. Under single target assumption, the classical criterion MSF (or ML) estimates the target position among detected positions as

$$(\hat{x}_{MSF}, \hat{y}_{MSF}) = \arg \max_{1\le j\le J} T_{MSF}(x_j, y_j). \quad (10)$$

C. Localization as a model selection problem

According to Eq. (10), the MSF localization criterion is supposed to choose from J test cells/positions the one that subspace is most likely to fit the observed data. However, as mentioned earlier, positions on the search domain are not illuminated by the same number of paths. Thus, their respective subspaces do not have similar dimensions. The ML criterion, given by Eq. (10), will naturally tend to favor subspaces with larger dimension, sometimes at the expense of the true one. This leads naturally to reformulate the single target localization problem as a model selection problem in which each position (x_j, y_j) stands for a model:

$$\mathcal{H}_j : \mathbf{z} = \mathbf{R}(x_j, y_j)\boldsymbol{\alpha} + \mathbf{n}, \tag{11}$$

where $\mathcal{H}_j$, $1 \leq j \leq J$ denotes the candidate model/position (x_j, y_j). This allows to adopt the well-known Bayesian Information Criterion (BIC) as model selection or localization criterion:

$$(\hat{x}_{BIC}, \hat{y}_{BIC}) = \arg \min_{1 \leq j \leq J} BIC(x_j, y_j), \tag{12}$$

where a robust form of the BIC, introduced in [15] has been chosen thanks to its consistency in both large number of samples N and high-SNR scenario:

$$\begin{aligned} BIC(x_j, y_j) = 2N \ln \hat{\sigma}_j^2 + 2M(x_j, y_j) \ln \left(\frac{N}{\pi}\right) \\ + (2M(x_j, y_j) + 2) \ln \left(\frac{\hat{\sigma}_s^2}{\hat{\sigma}_j^2}\right). \end{aligned} \tag{13}$$

Here $\hat{\sigma}_j$ is an estimator of the noise variance under the model j whose value is calculated as

$$\hat{\sigma}_j^2 = \frac{\|\mathbf{z} - \mathbf{P}(x_j, y_j)\mathbf{z}\|_2^2}{N}, \tag{14}$$

and

$$\hat{\sigma}_s^2 = \frac{\|\mathbf{z}\|_2^2}{N}, \tag{15}$$

denotes the additional scaling factor intended to handle the criterion consistency [15]. It is easy to see that contrary to the MSF criterion, the BIC in Eq. (13) enables to take into account each model complexity, hence penalizing the positions with large number of paths that overfit observed data. Using the BIC in that manner shall enable to solve the problem raised by the heterogeneity of the number of paths/model order among the different positions in localization problem.

III. Multipath selection algorithm

The BIC considered in the previous section enables to compare models of different dimensions in which each model corresponds to a different position. It does not, nevertheless, provide any clue on the way to select the number of paths for a given position. Indeed, the ray tracing simulation provides all possible propagation paths for a given urban scene configuration, *i.e.* a maximum bound on the number of paths. However exploiting all these paths for each position model would not be judicious for localization problem. Indeed, first, as discussed earlier, considering too many paths for each model increases the number of strongly correlated signal vectors between different subspaces, then can lead to localization ambiguities. Moreover, it can be observed that some of modeled paths may be in fact too weak due to multiple loss propagation factor or because they are unresolved and may interfere destructively with each other. This results in a discrepancy between the ray tracing number of paths and the effective number of informative paths. In the latter case, applying the BIC localization criterion, as in Eq. (13), can considerably penalize positions which do not actually have as many paths as in the model. Therefore, one needs to restrict the number of paths of each position model so as to better fit the reality.

To do this, one possibility is to select the most relevant path subset according to the observed data, given the ray tracing paths of each cell/position. Although this can be done by a model selection criterion like the BIC, the number of candidate models explodes since one needs to compare all possible combinations of paths. In order to make the problem computationally tractable, we propose here to use the well-known Orthogonal Least Squares (OLS) greedy algorithm, which consists in iteratively selecting paths in the ray tracing dictionary in order to get a sparse approximation of the observed data.

Concretely, let $\mathcal{I}$ denote the set of all indices i of columns/paths $\mathbf{r}_i$ of the ray tracing dictionary $\mathbf{R}$ of any position (x, y). Each iteration k consists in selecting path of indice i_k that minimizes the residual energy when combined with all previously selected paths, indices of which are contained in the set $\mathcal{S}_{k-1}$. According to [14], the OLS criterion is given by

$$i_k = \arg \max_{i \in \mathcal{I} \setminus \mathcal{S}_{k-1}} \frac{\left|\boldsymbol{\delta}_{k-1}^H \mathbf{r}_i\right|^2}{\left\|\mathbf{P}_{\mathcal{S}_{k-1}}^{\perp} \mathbf{r}_i\right\|_2^2}, \tag{16}$$

where

$$\mathbf{P}_{\mathcal{S}_k}^{\perp} = \mathbf{I} - \mathbf{P}_{\mathcal{S}_k} = \mathbf{I} - \tilde{\mathbf{R}}_k \left(\tilde{\mathbf{R}}_k^H \tilde{\mathbf{R}}_k\right)^{-1} \tilde{\mathbf{R}}_k^H, \tag{17}$$

and

$$\boldsymbol{\delta}_k = \mathbf{z} - \mathbf{P}_{\mathcal{S}_k}\mathbf{z} = \mathbf{P}_{\mathcal{S}_k}^{\perp}\mathbf{z}. \tag{18}$$

The latter denotes the residual obtained by projecting the data onto the orthogonal complement subspace of $\mathcal{S}_k$. The algorithm is supposed to run until a certain stopping rule is satisfied. Instead of setting a maximum number of paths for each position and thus the number of OLS iterations, we adopt again the BIC as the stopping rule, where it is thus applied here to limit the number of paths of one position. This procedure shall enable to solve the problem of selecting the effective number of paths for a given position. By doing this, goodness-of-fit is balanced with the model complexity: when the added path does not contribute enough to diminish the residual, the OLS stops. This procedure is applied for each position/cell (x, y) of the search domain. The proposed OLS-BIC procedure for multipath selection is summarized in Table 1.

Algorithm 1: Multipath selection OLS-BIC algorithm

Data: $\mathbf{z}$, $\{\mathbf{R}(x_j, y_j)\}_{1\leq j\leq J}$

Result: $\left\{\tilde{\mathbf{R}}(x_j, y_j)\right\}_{1\leq j\leq J}$

$\hat{\sigma}_s^2 \leftarrow \frac{\|\mathbf{z}\|_2^2}{N}$;

for j = *1 to* J **do**

  $\mathbf{r}_i = (\mathbf{R}(x_j, y_j))_i$, $\mathcal{I} \leftarrow \{i\}_{1\leq i\leq M(x_j,y_j)}$, $\tilde{\mathbf{R}}_k = \emptyset$;

  $\mathbf{P}_{\mathcal{S}_0} = \mathbf{I}$, $\mathcal{S}_0 \leftarrow \emptyset$, $\boldsymbol{\delta}_0 = \mathbf{z}$, $BIC_0 \leftarrow \infty$, $k \leftarrow 0$;

  while $BIC_k < BIC_{k-1}$ **do**

    $k \leftarrow k + 1$;

    $i_k \leftarrow \arg\max_{i\in\mathcal{I}\setminus\mathcal{S}_{k-1}} \frac{\left|\boldsymbol{\delta}_{k-1}^H \mathbf{r}_i\right|^2}{\left\|\mathbf{P}_{\mathcal{S}_{k-1}}^{\perp}\mathbf{r}_i\right\|_2^2}$;

    $\mathcal{S}_k = \mathcal{S}_{k-1} \cup \{i_k\}$;

    $\tilde{\mathbf{R}}_k \leftarrow \left[\tilde{\mathbf{R}}_{k-1} \quad \mathbf{r}_{i_k}\right]$;

    $\mathbf{P}_{\mathcal{S}_k} \leftarrow \tilde{\mathbf{R}}_k \left(\tilde{\mathbf{R}}_k^H \tilde{\mathbf{R}}_k\right)^{-1} \tilde{\mathbf{R}}_k^H$;

    $\boldsymbol{\delta}_k \leftarrow \mathbf{z} - \mathbf{P}_{\mathcal{S}_k}\mathbf{z} = \mathbf{P}_{\mathcal{S}_k}^{\perp}\mathbf{z}$;

    $\hat{\sigma}_k^2 \leftarrow \frac{1}{N}\left\|\boldsymbol{\delta}_k\right\|_2^2$;

    $BIC_k \leftarrow 2N \ln \hat{\sigma}_k^2 + 2k \ln\left(\frac{N}{\pi}\right)$

    $+(2k+2) \ln\left(\frac{\hat{\sigma}_s^2}{\hat{\sigma}_k^2}\right)$;

  end

  $\tilde{\mathbf{R}}(x_j, y_j) = \tilde{\mathbf{R}}_k$;

end

IV. Experimental results

We propose here an experiment in order to assess the performance of proposed solutions in terms of localization performance compared to other existing localization schemes. The set up is described in the following section.

A. Measurement setup

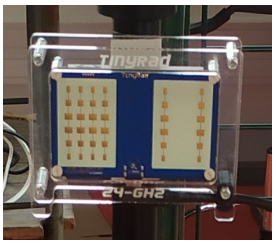

Fig. 1: The radar system [16]

1) Measuring equipment: the radar system used for the experiment is the EVAL-TINYRAD FMCW developed by Analog Devices [16], shown in Fig. 1. It integrates a linear array of $Q = 4$ receiving antennas where the element spacing is one-half of the wavelength. The signal $s(t)$ is emitted by a single antenna, consists of chirp pulses with carrier frequency $f_c = 24.05$ GHz and bandwidth $B = 235$ MHz, thus results in range resolution $\Delta_r = c/2B = 0.65$ m. The pulse repetition interval PRI and the number of pulses N_p are set to 200 µs and 400 pulses respectively in order to both guarantee no range migration and a good Doppler resolution ($\Delta_v = 0.07$ m/s) to separate the target contribution from fixed echoes.

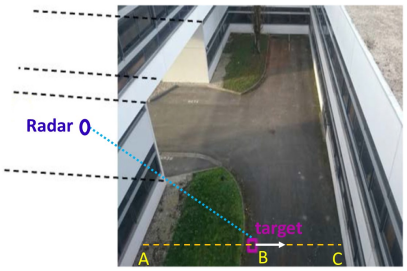

Fig. 2: A photo of the urban scene configuration.

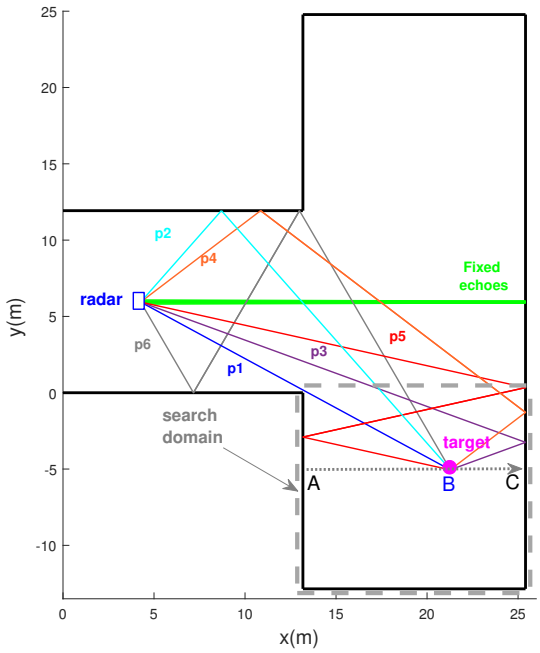

Fig. 3: The ray tracing simulation performed for the experiment scenario.

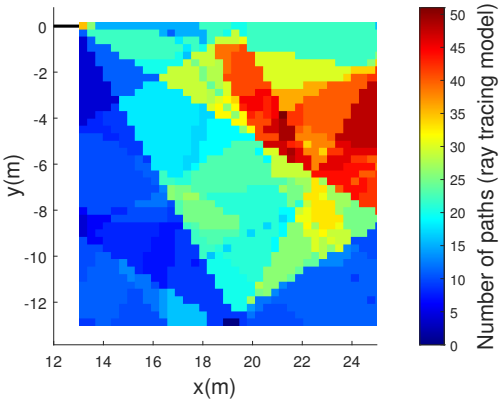

Fig. 4: The map of number of multipaths of each test cell/position in the search domain (ray tracing simulation).

2) Experiment scenario: we consider an urban scene as displayed in Fig. 2. The radar system is placed at the coordinates $(4.26; 5.94)$. At first, the target, in this case a pedestrian, is located at $A(13.18, -5.05)$ which is in NLOS with respect

to the radar. Then he starts moving up to $C(25.41, -5.05)$ where he appears in LOS for the first time at the point $B(20.58, -5.05)$. The radar system records the signal during 6.16 sec that covers the total target trip duration.

3) Ray tracing simulation: only the rough scene 2D geometry is transcribed to the simulator (Fig. 3) so as to perform ray tracing simulation. The latter is intended to build the multipath model of each test cell in the search domain, also defined in Fig. 3. To do this, one needs to divide the search domain into 0.3×0.3 m cells that is approximately half of the aforementioned radar range resolution. Then for each cell (x, y), the ray tracing simulation is run and rays information is retrieved for constructing the multipath dictionary $\mathbf{R}(x, y)$ according to Section II. Here the maximum number of ray reflections in the simulation is set to 4 due to the fact that path may suffer from severe attenuation beyond this value; the path maximum range is limited to 76.5 m because of the maximum range supported by the radar system. After building all test cells model, the map of number of paths in the search domain is drawn in Fig. 4, where different illuminated zones can be identified: as mentioned earlier, it can be observed that the number paths is highly heterogeneous from a zone to another.

4) Signal preprocessing: the radar system output yields the sampled beat signal of each received channel, stored in a fast-time-slow-time matrix in which classical 2D-FFT processing can be applied. Here fixed echoes are cancelled by simply filtering out all zero-Doppler components from the signal spectrum. Then, as it is not intended to use Doppler information in our data model, the range-dependent only data vector $\mathbf{z}_q$ can be extracted from the 2D-FFT matrix by selecting, for each range bin, the corresponding Doppler bin with highest peak. This can be done under the assumption that each multipath only occupies a single range-Doppler bin with dominant magnitude. Thus, displaying the data vector over time yields the target range-time profile as shown in Fig. 5a.

B. Localization results

In this section, we compare the localization results of several localization schemes on both simulated an real data: 1) The classical MSF localization criterion, described in Section II-B; 2) The MSF localization criterion coupled with the path selection procedure for maximizing detection probability proposed in [9], that we call MAX-PD; 3) The BIC localization criterion (cf. Section II-C) based on ray tracing model, called RT-BIC; 4) The MSF localization criterion coupled with the path selection procedure OLS-BIC (cf. Section III), called OLS-BIC; 5) The BIC localization criterion coupled with the path selection procedure OLS-BIC, called OLS-BIC^2. It should be highlighted that the detection test in Eq. (8) is first performed for all positions with $P_{FA} = 10^{-6}$. Then only detected positions are considered for localization problem. Especially, the detection of LOS positions is assumed to depend only on the direct path SNR as in classical radar detection problem. In order to assess the robustness of these localization schemes, we have also done 20 Monte Carlo (MC) of the proposed experiment in which both random target fluctuation loss, assumed to follow the Swerling 3 model and the CWGN are considered. A realization of the target range-time profile is shown in Fig. 5d.

Fig. 5 shows the simulation localization error curves of the considered localization schemes averaged over 20 MC simulations. It can be stated that applying the BIC localization criterion RT-BIC, the OLS-BIC path selection procedure, or coupling them together (OLS-BIC^2) allows to improve the localization performance compared with the classical MSF localization scheme, notably in the NLOS zone where the number of paths is quite small. This improvement can be also observed in real data localization results in Fig. 5f. Indeed, real data localization error curves seem to present larger values and be more distinct within each other. This can be explained first by the fact that simulated data error curves have been averaged over MC simulations, and second of course real data are more involved. Especially, the OLS-BIC^2 scheme reveals to be more robust in zones with larger number of paths compared to the RT-BIC. This complies with our remark in Section III that is the OLS-BIC enables to refine the number of paths of each position and hence makes the BIC penalty more relevant. We also want to highlight that the MAX-PD procedure, designed for optimal detection problem, is not efficient for localization. Its large error can be explained by the fact that when certain paths are already too strong, it tends to discard other weaker but actually informative paths that help to dissociate the target position and false estimated position.

Fig. 5b and Fig. 5e show the number of paths of the estimated subspace considered by each localization scheme in simulated and real data, respectively. Despite a smaller number of exploited paths compared with the MSF which uses the whole ray tracing dictionary, both OLS-BIC and OLS-BIC^2 still yield better localization results. Besides, the OLS-BIC procedure tends to select more informative paths than the MAX-PD one. It follows that the OLS-BIC procedure offers a reasonable way to select paths for the localization problem.

V. Conclusion

In this paper, we introduced two solutions to deal with two problems that affect the performance of in locating a single NLOS target: heterogeneity of number of paths in the search domain and selecting the informative paths for the localization problem. Both simulated and experimental localization results show that the target position is more accurately estimated using the BIC localization criterion coupled with the proposed OLS-BIC multipath selection procedure compared to the classical localization scheme.

References

[1] A. Sume, M. Gustafsson, M. Herberthson, A. Janis, S. Nilsson, J. Rahm, A. Orbom, "Radar Detection of Moving Targets Behind Corners," in IEEE Transactions on Geoscience and Remote Sensing, vol. 49, no. 6, pp.2259-2267, 2011.

[2] T. Johansson, Å. Andersson, M. Gustafsson and S. Nilsson, "Positioning of moving non-line-of-sight targets behind a corner," 2016 European Radar Conference (EuRAD), 2016, pp. 181-184.

[3] O. Rabaste, E. Colin-Koeniguer, D. Poullin, A. Cheraly, J.F. Petex, H.K. Phan, "Around-the-corner radar: detection of a human being in non-line of sight", IET Radar, Sonar & Navigation, 2015, 9, (6), pp. 660–668.

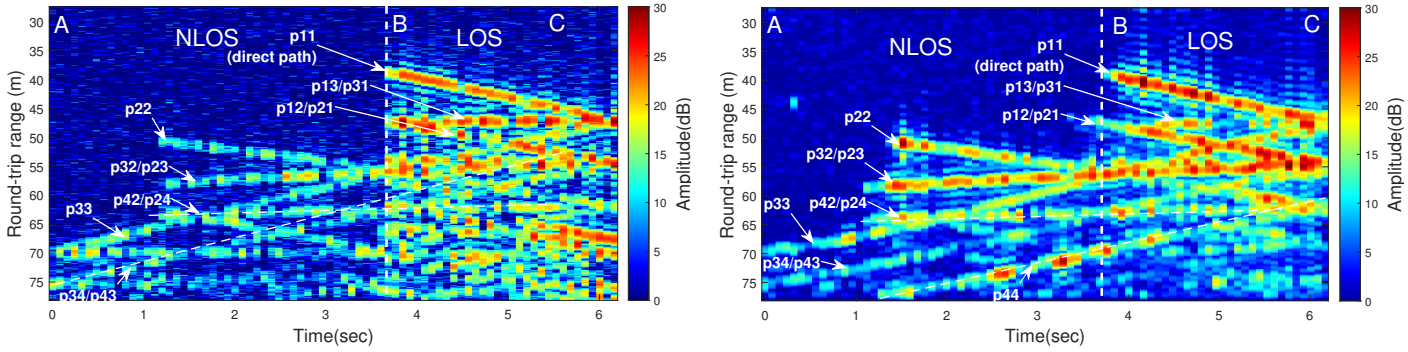

(a) Range-time profile (simulation)

(d) Range-time profile (real data)

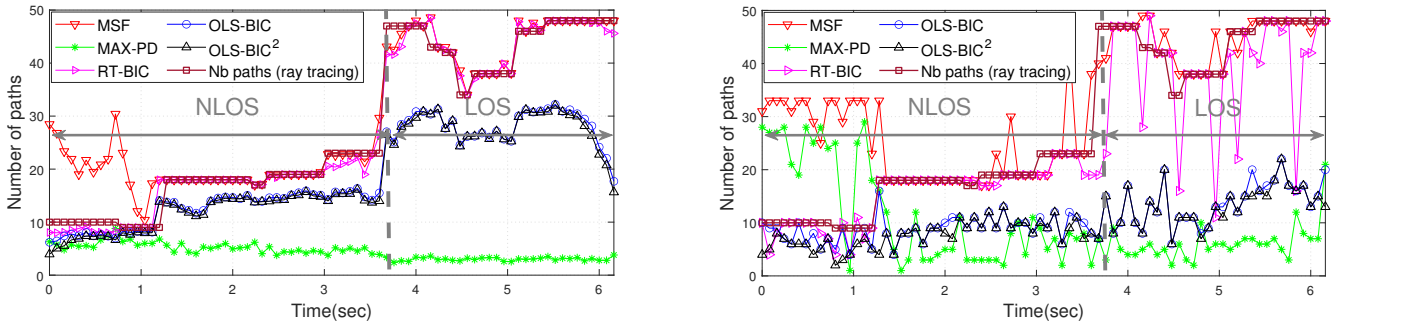

(b) Number of paths of the estimated position (simulation)

(e) Number of paths of the estimated position (real data)

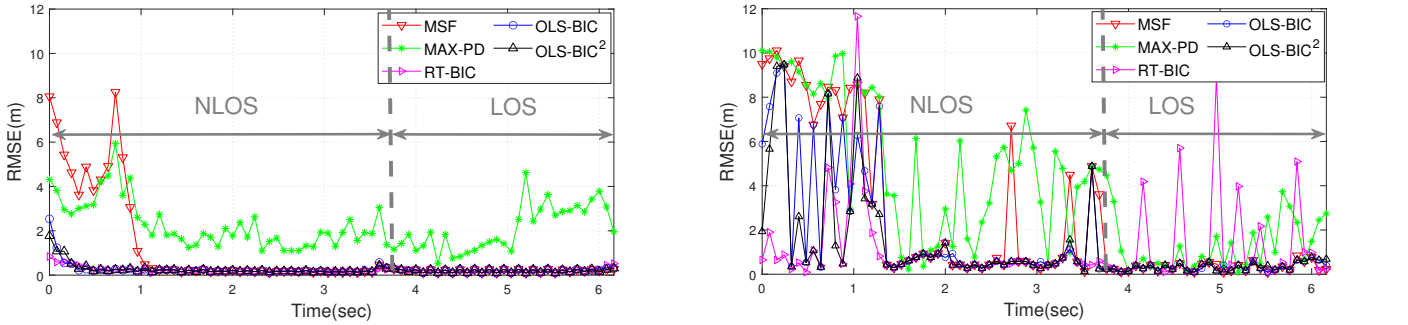

(c) Localization error (simulation)

(f) Localization error (real data)

Fig. 5: Target range-time profile, number of selected paths of the estimated position and localization error along the target trajectory for several localization scheme. (a), (b), (c): simulated data. (c), (d), (e): real data.

[4] Q. Zhao, G. Cui, S. Guo, W. Yi, L. Kong and X. Yang, "Millimeter Wave Radar Detection of Moving Targets Behind a Corner," 2018 21st International Conference on Information Fusion (FUSION), pp. 2042-2046, 2018.

[5] H. Du, C. Fan, Z. Chen, C. Cao, and X. Huang, "NLOS Target Localization with an L-Band UWB Radar via Grid Matching," Progress In Electromagnetics Research M, Vol. 97, 45-56, 2020.

[6] N. Scheiner, F. Kraus, F. Wei, B. Phan, F. Mannan, N. Appenrodt, et al, "Seeing Around Street Corners: non-line-of-sight detection and tracking in-the-wild using doppler radar," in proc. IEEE Conf. Comput. Vis. Pattern Recog., Los Angeles, CA, USA, 2019.

[7] S. Fan, Y. Wang, G. Cui, S. Li, S. Guo, M. Wang, L. Kong, "Moving Target Localization Behind L-shaped Corner With a UWB Radar," 2019 IEEE Radar Conference (RadarConf), 2019, pp. 1-5.

[8] S. Li, S. Guo, J. Chen, X. Yang, S. Fan, C. Jia, G. Cui, H. Yang, "Multiple Targets Localization Behind L-Shaped Corner via UWB Radar," in IEEE Transactions on Vehicular Technology, vol. 70, no. 4, pp. 3087-3100, 2021.

[9] K. Thai, O. Rabaste, J. Bosse, D. Poullin, I. Hinostroza, T. Letertre, T. Chonavel, "Detection–Localization Algorithms in the Around-the-Corner Radar Problem," in IEEE Transactions on Aerospace and Electronic Systems, vol. 55, no. 6, pp. 2658-2673, 2019.

[10] L. L. Scharf and B. Friedlander, "Matched subspace detectors," in IEEE Transactions on Signal Processing, vol. 42, no. 8, pp. 2146-2157, 1994.

[11] A. J. Weiss, "Direct Geolocation of Wideband Emitters Based on Delay and Doppler," in IEEE Transactions on Signal Processing, vol. 59, no. 6, pp. 2513-2521, 2011.

[12] B. Pham, O. Rabaste, J. Bosse, I. Hinostroza and T. Chonavel, "On the reduction of localization ambiguities of hidden target in the around-the-corner radar," CIE Conference on Radar, 2021 (in press).

[13] G. Schwarz, Estimating the Dimension of a Model. Annals of Statistics, 6, 461-464, 1978.

[14] S. Chen, S. A. Billings, and W. Luo, "Orthogonal least squares methods and their application to non-linear system identification," International Journal of control, vol. 50, no. 5, pp. 1873–1896, 1989.

[15] P. Gohain, M. Jansson, "Scale-Invariant and consistent Bayesian information criterion for order selection in linear regression models," Signal Processing, Volume 196, 2022.

[16] https://www.analog.com/en/design-center/evaluation-hardware-and-software/evaluation-boards-kits/eval-tinyrad.html